ACCEPTED MANUSCRIPT

Low-temperature low power PECVD synthesis of vertically aligned graphene

To cite this article before publication: Shahzad Hussain *et al* 2020 *Nanotechnology* in press https://doi.org/10.1088/1361-6528/ab9b4a

Manuscript version: Accepted Manuscript

Accepted Manuscript is “the version of the article accepted for publication including all changes made as a result of the peer review process, and which may also include the addition to the article by IOP Publishing of a header, an article ID, a cover sheet and/or an ‘Accepted Manuscript’ watermark, but excluding any other editing, typesetting or other changes made by IOP Publishing and/or its licensors”

This Accepted Manuscript is **© 2020 IOP Publishing Ltd**.

During the embargo period (the 12 month period from the publication of the Version of Record of this article), the Accepted Manuscript is fully protected by copyright and cannot be reused or reposted elsewhere.
As the Version of Record of this article is going to be / has been published on a subscription basis, this Accepted Manuscript is available for reuse under a CC BY-NC-ND 3.0 licence after the 12 month embargo period.

After the embargo period, everyone is permitted to use copy and redistribute this article for non-commercial purposes only, provided that they adhere to all the terms of the licence https://creativecommons.org/licences/by-nc-nd/3.0

Although reasonable endeavours have been taken to obtain all necessary permissions from third parties to include their copyrighted content within this article, their full citation and copyright line may not be present in this Accepted Manuscript version. Before using any content from this article, please refer to the Version of Record on IOPscience once published for full citation and copyright details, as permissions will likely be required. All third party content is fully copyright protected, unless specifically stated otherwise in the figure caption in the Version of Record.

View the article online for updates and enhancements.

This content was downloaded from IP address 161.116.100.31 on 11/06/2020 at 11:20

Low-temperature low power PECVD synthesis of vertically aligned graphene

Shahzad Hussain[a,b] , *Eva Kovacevic*[a*], *Johannes Berndt*[a], *Neelakandan M Santhosh*[c,d], *Cédric Pattyn*[a], *Ana Dias*[a,e], *Thomas Strunskus*[f], *Mohamed-Ramzi Ammar*, [g,h], *Andrea Jagodar*[a], *Mireille Gaillard*[a], *Chantal Boulmer-Leborgne*[a], *Uroš Cvelbar*[c]

[a] GREMI, UMR 7344, CNRS & Université d'Orléans, 45067 Orleans Cedex 2, France, EU.
[b] Nanotechnology & Integrated Bio-Engineering Centre (NIBEC), Ulster University, Shore Road, Newtownabbey BT37 0QB, United Kingdom.
[c] Jožef Stefan Institute, Jamova cesta 39, SI1000 Ljubljana, Slovenia, EU
[d] Jožef Stefan International Postgraduate School, Jamova cesta 39, SI-1000 Ljubljana, Slovenia, EU
[e] Instituto de Plasmas e Fusão Nuclear, Instituto Superior Técnico, Universidade de Lisboa, 1049-001 Portugal, EU.
[f] Multicomponent Materials, Institute for Materials Science, Kiel University, Kaiserstr. 2, D-24143, Kiel, Germany, EU.
[g] ICMN UMR7374, CNRS & Université d'Orléans, 45071, Orléans Cedex 2, France, EU.
[h] CEMHTI UPR3079, CNRS, Univ. Orleans, F-45071, Orleans Cedex 2, France, EU.

*Corresponding author. Tel: +33238494606. E-mail: eva.kovacevic@univ-orleans.fr

Accepted Manuscript

Abstract

The need for 2D vertical graphene nanosheets (VGNs) is driven by its great potential in diverse energy, electronics, and sensor applications, wherein many cases a low-temperature synthesis is preferred due to requirements of the manufacturing process. Unfortunately, most of today's known methods, including plasma, require either relatively high temperatures or high plasma powers. Herein, we report on a controllable synthesis of VGNs at a pushed down low-temperature boundary for synthesis, the low temperatures (450 ºC) and low plasma powers (30 W) using capacitively coupled plasma (CCP) driven by radio-frequency power at 13.56 MHz. The strategies implemented also include unrevealing the role of Nickel (Ni) catalyst thin film on the substrates (Si/Al). It was found that the Ni catalyst on Si/Al initiates the nucleation/growth of VGNs at 450 °C in comparison to the substrates without Ni catalyst. With increasing temperature, the graphene nanosheets become bigger in size, well-structured and well separated. The role of Ni catalysts is hence to boost the growth rate, density, and quality of the growing VGNs. Furthermore, this CCP method can be used to synthesize VGNs at the lowest temperatures possible so far on a variety of substrates and provide new opportunities in the practical application of VGNs.

Keywords: VGNs, PECVD, Raman, XPS, NEXAFS

Accepted Manuscript

1. Introduction

Vertical graphene nanosheets (VGNs), also referred to as vertically-oriented graphene nanosheets (VOGN) or carbon nanowalls (CNWs) are two-dimensional graphitic platelets which are typically oriented vertically on a substrate [1]. Rising interest in the synthesis and application of VGNs emanates from their unique characteristics such as non-stacking morphology, high-aspect-ratio, sharp edges, and high-density reticular arrangement, etc. [2–4]. Besides this, excellent electrical and mechanical properties of VGNs and their derivatives enabling their applicability in enormous fields, including supercapacitor, battery electrodes, power sources, field emitters, flexible electronics, gas sensors, and catalyst supporters [5–10]. An individual VGN typically consist of few stacked graphene layers having a thickness of several few nanometres with lateral and vertical dimensions of hundreds of nanometres to tens of micrometres. With few exceptions where chemical vapour deposition (CVD), and sputtering techniques for the synthesis of VGNs are used, plasma-enhanced chemical vapour deposition (PECVD) methods are considered as the emerging techniques for building VGNs. Compared to other techniques, PECVD techniques offer a low-temperature synthesis of VGNs with controlled growth and morphology at a large scale. The structure and morphology of VGNs can be influenced by plasma sources and parameters such as substrate temperature, feedback gas type and composition, operating pressure and plasma power used for the synthesis process [11,12].

In a PECVD system during the growth of VGNs, the precursor gas (generally hydrocarbons) undergo inelastic collisions with the electrons in the plasma to form different plasma species. It has been already reported that the VGNs can grow on the substrate without the presence of catalyst particles, which indicates that the precursor dissociation by plasma and interaction of plasma species to the substrate surface plays a key role for the growth of VGNs. Thus, several studies have been carried out for successfully synthesising VGNs using various plasma sources such as radiofrequency inductively coupled plasma (RFICP) [13], microwave plasma [14], DC plasma [15], RF capacitively coupled plasma (RFCCP) assisted by radical injection [16], helicon plasma, and electron beam excited plasma (EBEP). Generally, a higher concentration of hydrogen atoms and carbon dimers (C_2 radicals) are needed for the growth of VGNs [17]. Carbon dimers produced by the radical recombination and subsequent dissociation of CH_x (x=1,2,3) radicals are playing a vital role in the nucleation of VGNs and hydrogen acts as the etching agent for the removal of amorphous carbon(a-C). It has been reported that microwave (MW) and ICP systems employed with CH_4/H_2 or $CH_4/H_2/Ar$ mixture have higher C_2 radical

Accepted Manuscript

density for the direct nucleation for the VGN growth. On the other hand, a CCP plasma effectively generates CH_3 radicals from the carbon precursor, but because of the deficiency of H atoms, CCP plasma by itself is not suitable for the growth of VGNs [18,19]. Thus, radical injection of H atoms and coupling of CCP with other plasma sources are used to provide sufficient H atoms for the growth of VGNs.

In addition to the plasma source, the most direct and controllable parameters in the PECVD process that can influence the growth and morphology of VGNs are plasma power and substrate temperature [19,20]. Several groups successfully synthesised VGNs by employing MW plasma with power in the range of 350W-16 kW at a substrate temperature between 350-700°C [2,21]. ICP plasmas with a power range from 400 W to 1000 W at substrate temperatures of 350-1100 °C have also been used for synthesising VGNs [21,22], as well as DC plasma and EBEP plasma sources by employing higher input power and temperature [23,24]. Most of all the reported VGN growth by CCP was assisted either by an external hydrogen source or by other plasma sources at different power (250-700 W) and temperature (500-700°C) [25–27]. The lowest temperature that has been used for the growth of VGNs so far is ~350°C using an ICPECVD system, where an external bias was added for the VGN growth [22]. In all other cases, the VGN growth was observed at a temperature above 500 °C by employing higher plasma power. Also, it has been demonstrated that higher temperatures and higher plasma power can corrugate the morphology of VGNs [28]. Therefore, the synthesis of VGNs at lower temperatures and lower power without using any additional plasma source or bias is still considered as the main challenge in the research of oriented graphene structures.

Even though VGNs can grow on the substrate without any addition of a catalyst, several researchers have taken the effort to investigate the effect of catalysts (e.g., Ni) on the growth of VGNs [29–31]. It has been reported that the low-temperature plasma assisted treatment improve the catalyst substrate interaction, reduce the catalyst particles mobility and thus influence the growth of such 2D and 3D materials [32]. Also, during the annealing of the substrate, the application of plasma-pre-treatment readily transform the catalyst layer and reduces the size of the catalyst nanoparticles, which drastically improves the homogeneity [32]. Thus, the hydrogen plasma treatment is almost considered as a standard pre-treatment, and several morphologies have been documented by this method [33]. On the other hand, an argon plasma, which is more effective than hydrogen plasma for the cleaning or etching, is very rarely used for the pre-treatments. Therefore, revealing the effect of Ar plasma pre-treatment on the substrate surface for the growth of VGNs can be beneficial for future applications.

Accepted Manuscript

Herein we are reporting a successful application of a radio frequency capacitively coupled plasma-enhanced chemical vapour deposition (RFCCPECVD) system at lower power and lower temperature for the synthesis of VGNs without using any additional plasma source. VGNS were synthesised in a cold wall CCPECVD reactor using a very low power of 30 W at a substrate temperature of 450 °C to 620 °C. The influence of Ni thin film on the growth rate and structure quality of VGNs was also investigated. We have investigated the effect of substrate temperature on the structural quality of VGNs using Raman spectroscopy and chemical composition analysis. NEXAFS spectroscopy was used to obtain chemical, structural and orientation information of the nanoscale samples. To our knowledge, a successful application of capacitively coupled plasma to synthesis VGNs using low power and temperature has not been reported so far.

2. Experimental Section

2.1. Synthesis of VGNs

The VGNs were synthesized using a cold-wall CVD by radio frequency capacitively coupled plasma (RFCCP) operated at 13.56 MHz RF power. The detailed scheme of experimental setup has been presented in our previous studies [33–37]. Silicon wafers covered with 200 nm thick aluminium (Al) are used as the substrate for synthesizing VGNs. A 10 nm thin Ni film was deposited by a precision etching coating system (PECS) onto the Si/Al to investigate the effect of catalytic materials on the growth of VGNs[31]. These values were chosen after several trial and error experiments and showed the best results. The substrate was transferred into the PECVD reactor, and the base pressure inside the reactor was kept below $4\cdot10^{-4}$ Pa. Substrates were pre-treated at different annealing temperatures (450 °C to 620 °C) with CCP plasma. Argon gas (10 sccm) was inserted to the chamber at a pressure of ~29 pa for the pre-treatment with a ramp time of (960 s to 1200 s) and held the conditions for 1800 s. Subsequently, a mixture of hydrogen (H_2) and ethylene (C_2H_4) with a flowrate of 40:20 sccm were introduced to the reactor at the pressure of ~100 pa and the growth of VGNs was performed for 900 s. For simplicity, the growth scheme of VGNs presented here is very similar to the growth of CNTs performed in previous studies [31,36].

2.2. Characterization techniques

Scanning electron microscopy (SEM) by a Zeiss-Supra device was used to examine the morphology of VGNs. Raman spectra were recorded to study the structural organization of the synthesised VGNs using a Renishaw InVia Reflex Spectrometer at an excitation wavelength

Accepted Manuscript

of 514.5 nm. The spectra were collected under a Leica DM2500 optical microscope (×50 objectives/N.A.= 0.75) and a grating of 1800 l/mm. The laser power in the sample was kept at around 0.5 mW to avoid any heating damage. The samples were analysed at three different spots. The elemental composition and orientation-dependent chemical properties of VGNs were analyzed by X-ray photoelectron spectroscopy (XPS) and Near Edge X-ray-absorption fine structure (NEXAFS) spectroscopy using the HE-SGM beam line with the PREVAC end station at the BESSY II electron storage ring in Berlin, Germany. The elemental depth information during the analysis was about 2 nm by measuring the high-resolution photoelectron lines of the different elements at the same constant kinetic energy [38].

3. Results and discussion

The SEM micrographs displayed in Figure 1 indicate a vertically standing morphology and uniform growth of VGNs on Si/Al and Si/Al/Ni substrates at different temperatures ranging from 450 to 620 °C. Even though the general morphology of VGNs is similar, the density, interlayer spacing, and thickness of VGNs are varying along with the temperature. A comparison between the growth of VGNs with and without the presence of a Ni catalyst suggests that the morphology of VGNs is different even for the same growth temperature. This could be related to differences in the nucleation steps evolving in the initial stages [31], where the nucleation of nanoislands during the growth of VGNs with Ni catalyst is faster than without Ni.

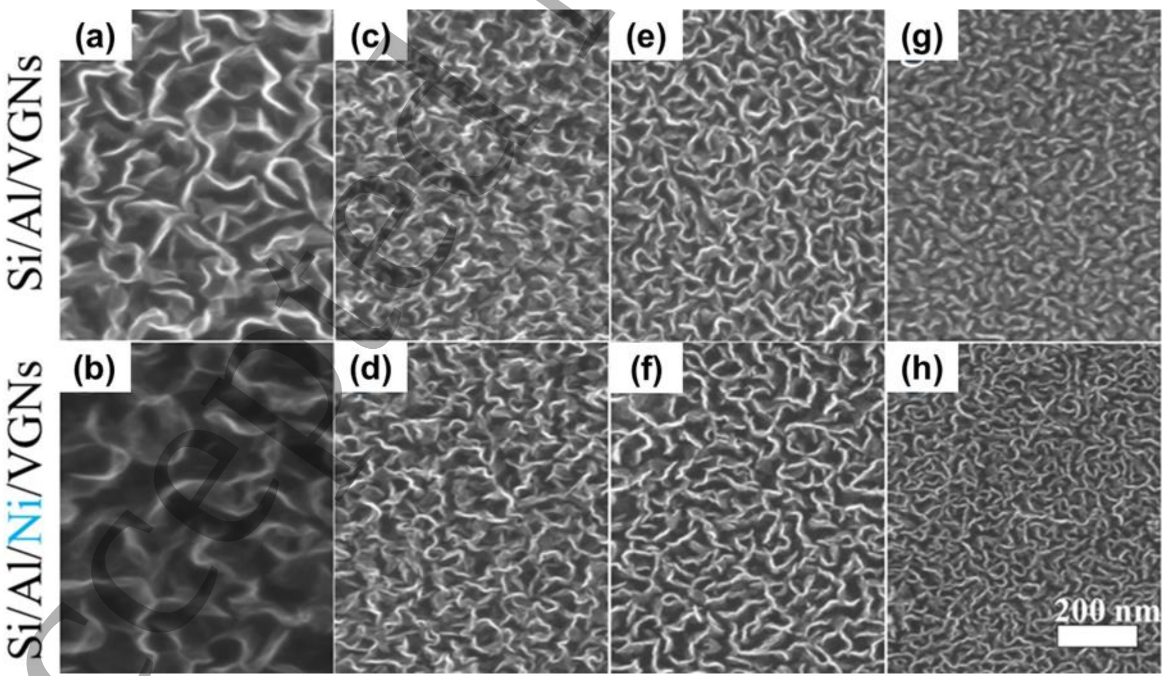

Figure 1. SEM images of VGNs obtained at 620 °C (a, b), 550 °C (c, d), 480 °C (e, f), 450 °C (g, h). scale bar is 200 nm for all figures.

Accepted Manuscript

At lower temperatures, nucleation and initial growth of densely packed nanosheets are occurring due to the longer surface residence time for the different plasma species; however, the possible migration of plasma species on the substrate surface at low temperature is lower than that at higher temperature and results in smaller lateral and vertical dimensions of VGNs at lower temperature. The lateral dimension of the individual nanosheets is increasing with the temperature and highly interconnected nanosheets are observed at higher temperatures.

Considering the fact that the density and interlayer spacing of the VGNs is varying with the growth temperature, the changes in the vertical dimension of the VGNs are also investigated. Figure 2 (a-d) exhibits the cross-sectional images of the VGNs grown at different temperatures. The height of VGNs on Si/Al increases from 130 nm to 270 nm for temperatures 480 °C to 620 °C, respectively. The addition of Ni catalyst enhances the growth of VGNs as the height reaches 150 nm to 500 nm for temperatures 480 °C to 620 °C, as displayed in figure 2 (e). The growth of VGNs observed on the Si/Al and Si/Al/Ni substrates at the lower temperature (480 °C) is having an almost similar growth rate of 520-600 nm/h. Hence with the increase in temperature to 620 °C, the growth rate of VGNs on Si/Al/Ni substrates (~2 μm/h) is two-times higher than on Si/Al (~1 μm/h). Since the plasma power is very low and maintained constant during the experiments, the effect of plasma heating of the substrate can be neglected. Thus, the changes in growth rate can be explained as a combined effect of growth temperature and catalyst particle. At lower growth temperature, the plasma species has high surface residence time with low mobility of the surface atoms. On the other hand, at higher temperatures, the migration of plasma generated species on the substrate surface is higher and favours the formation of interconnected stable nanostructures by surface chemical reactions. This results in the formation of well-aligned highly interconnected VGNs at higher temperatures. The presence of the Ni catalyst is enhancing the surface diffusion of the hydrocarbon species on the surface for the initial growth of graphene layers and promotes a higher growth rate on the Si/Al/Ni substrates. In order to gain a better understanding of the influence of temperature and Ni catalyst on the structural organization and chemical composition of the VGNs, the samples were further analysed with different surface analytical techniques.

Accepted Manuscript

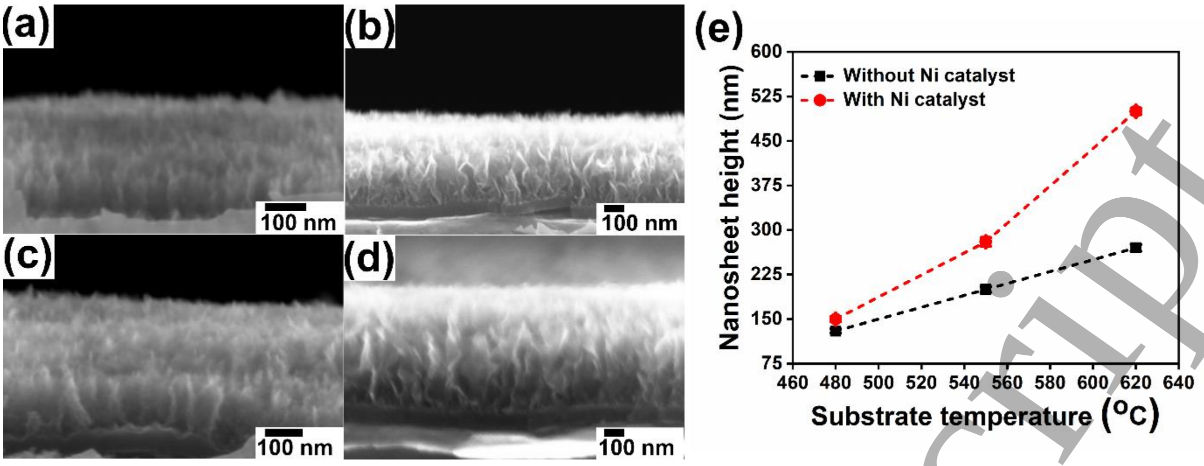

Figure 2. SEM images of VGNs height comparison on Si/Al {(a) at 480 °C, (b) at 620 °C}, on Si/Al/Ni {(c) at 480 °C, (d) at 620 °C}, (e) variation of VGNs height with respect to growth temperature.

The inner structural arrangement of the VGNs synthesised on different substrates at different temperatures was analysed by Raman spectroscopy. Figure 3 (a and b) displays normalised Raman spectra of VGNs grown on substrates with and without Ni thin films at different temperatures. The spectra are composed of several bands; most importantly, the D band located at ~1350 cm^{-1} attributed to the A_{1g} breathing mode of six-atom rings at the 1st Brillouin zone boundary K or K'. Due to the conservation of momentum, it becomes active only in the presence of defects. The G band at ~1581 cm^{-1} corresponds to the one-phonon Raman scattering process at the 1st Brillouin zone centre and consists of the collective in-plane bond stretching of carbon atoms (E_{2g} symmetry) [39,40]. The D' band at 1622 cm^{-1} is also a defect-induced phonon mode near the 1st Brillouin zone centre. The G'(2D) band at ~2700 cm^{-1} and the G'' (2D') band at ~3240 cm^{-1} are respectively the second orders of the D and D' bands originating from the scattering by two phonons with opposite wave vectors, and therefore they are always active by symmetry [41]. The D+D' band observed at ~2940 cm^{-1} corresponds to the combination of phonons and also requires defects for its activation [42].

As the growth temperature is increasing, the recorded Raman spectra undergo several changes, which indicates the structural modification of the resulting VGNs. Figure 3 (c) and (d) display the evolution of the full width at half maximum FWHM of D and G'(2D) as a function of the growth temperature. Both parameters, which are the fundamental characteristics of the local structural order, are decreasing with a temperature towards minimum values suggesting the increased structural ordering of VGNs with increased growth temperature. Figure 3 (e) exhibits the changes in the I_{2D}/I_G ratio, which continuously increases with an increase in temperature. It

Accepted Manuscript

is the characteristic behaviour for an increase in the concentration of polyaromatic carbons. Moreover, the G and D' bands are merged and seen as a single band located at ~1600 cm^{-1} for the VGNs grown at 450 °C and 480 °C, which is due to the lower structural order.

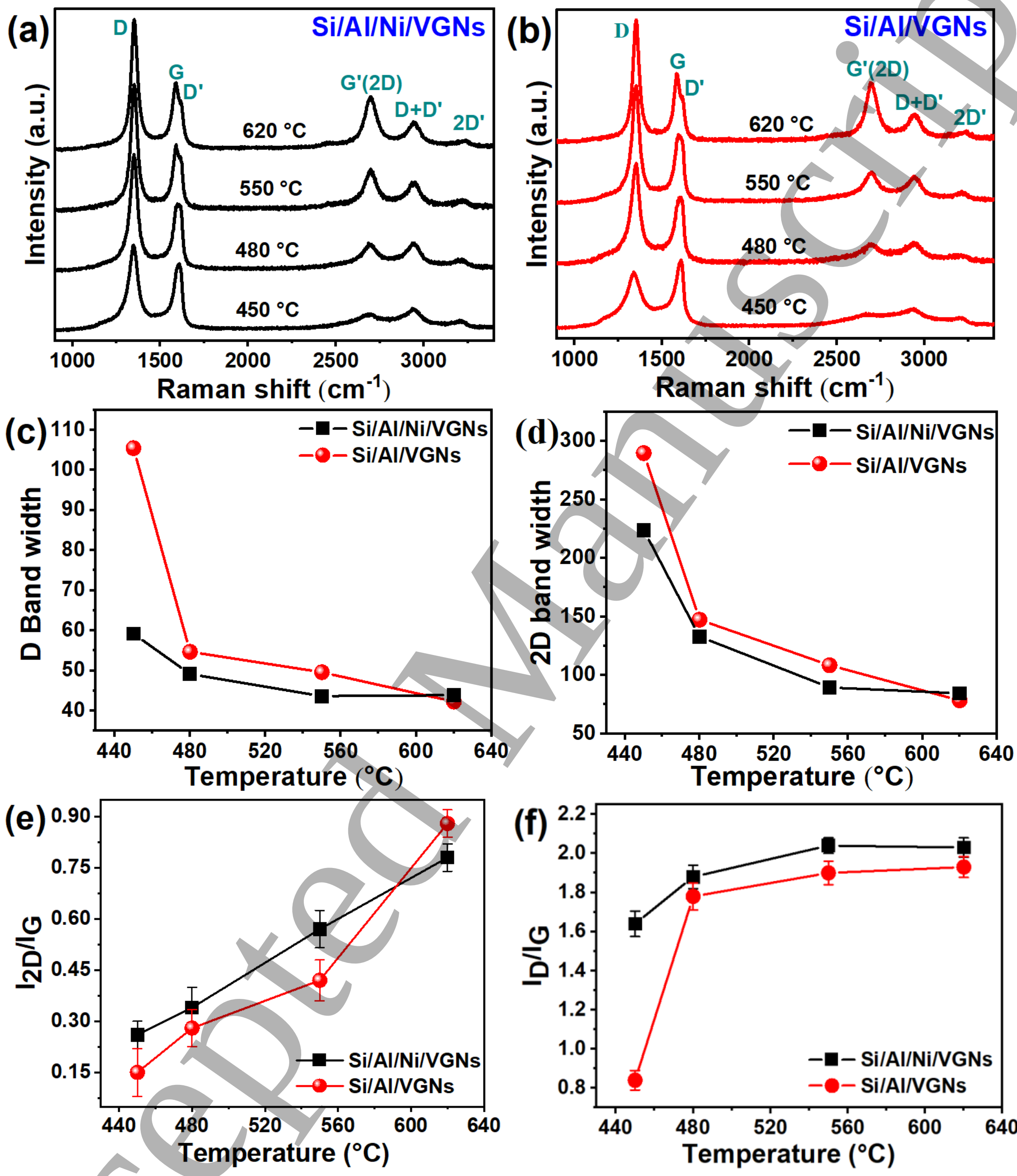

Figure 3. Raman spectra of VGNs grown at different temperatures (a) with Ni thin film (b) without Ni thin film, (c, d) Full widths at half maximum FWHM(D) and FWHM(2D) for different growth temperatures (e, f) Raman intensities comparison for different growth temperatures.

Accepted Manuscript

For higher growth temperatures (550 °C and 620 °C), the G band position undergoes a downshift towards lower wavenumbers leading to a clear distinction of D' band. All these variations are in good agreement with the literature regarding the characterization of sp^2 carbon-based materials with an increasing degree of ordering [19,43,44]. Figure 3(f) represents the variation of the I_D/I_G with the growth temperature, which varies with the type and concentration of the introduced defects [42,45,46] and exhibits opposite behaviour compared to what is usually seen in the literature [47]. In this specific range of structural ordering, this parameter is expected to continually decrease with the increase in growth temperature. Generally, defect density characterized by different geometries is quantified by Raman scattering via the number of active areas around borders or point-like defects with respect to the total area of the laser spot. Therefore, the variation of I_D/I_G provides a measure of the crystallite size L_a or a determination of the average distance between point-like defects L_D. In the present work, there is a fundamental difference in the orientation (vertical growth) of the analysed graphene nanosheets. This configuration results in the exposure of the laser spot to a large number of graphene edges vertically aligned that satisfy the momentum conservation leading to the full activation of the D band. Therefore, since the D band is the breathing mode of polyaromatic carbon, increasing the ordering of graphene nanosheets with the growth temperature leads to an increase of its intensity similar to what could be observed for its second-order band G'(2D) active by symmetry. Its asymptotic behaviour (or possible decrease) can be explained by the increase of the spacing between the walls in the area illuminated by the laser spot. One must, therefore, be careful about interpreting the Raman spectra based only on the I_D/I_G ratio. This also means that all the relationships found in literature allowing the determination of in-plane crystallite size (L_a or L_d) based on the I_D/I_G, should definitely not be used in the case of vertically aligned graphene nanosheets [48–50]. The SEM images and Raman analysis confirm that VGNs start to grow at the lowest temperature of 450 °C and show a relatively well-organized structure at 550 °C when Ni catalyst has been used whereas without catalyst the growth starts at a temperature of about 480 °C and a well-organized structure is obtained at 620 °C.

Chemical compositions of the grown VGNs at different temperatures were investigated with XPS. Figure 4(a) shows XPS survey scans of the samples. The analysis suggests the existence of only two elements in VGNs, namely carbon and oxygen. Samples show different O 1s to C 1s ratios for VGNs grown without Ni catalyst and with Ni catalyst. In both cases, the appearance of O 1s lines is probably due to chemical reactions of structural defects and dangling bonds upon exposure to the ambient. The analysis also indicates the reduction of

Accepted Manuscript

oxygen functional groups and an increase in carbon content with an increase in the growth temperature as represented in figure 4(b), possibly due to an increase of the crystallinity of the VGNs structure. Figure 4(c) shows the high resolution of deconvoluted C 1s spectra of VGNs grown with Ni catalyst at 550 °C. For the deconvolution of the C 1s line, the position at 284.5 eV was taken as a reference, which is assigned to regular graphitic carbon atoms [51,52].

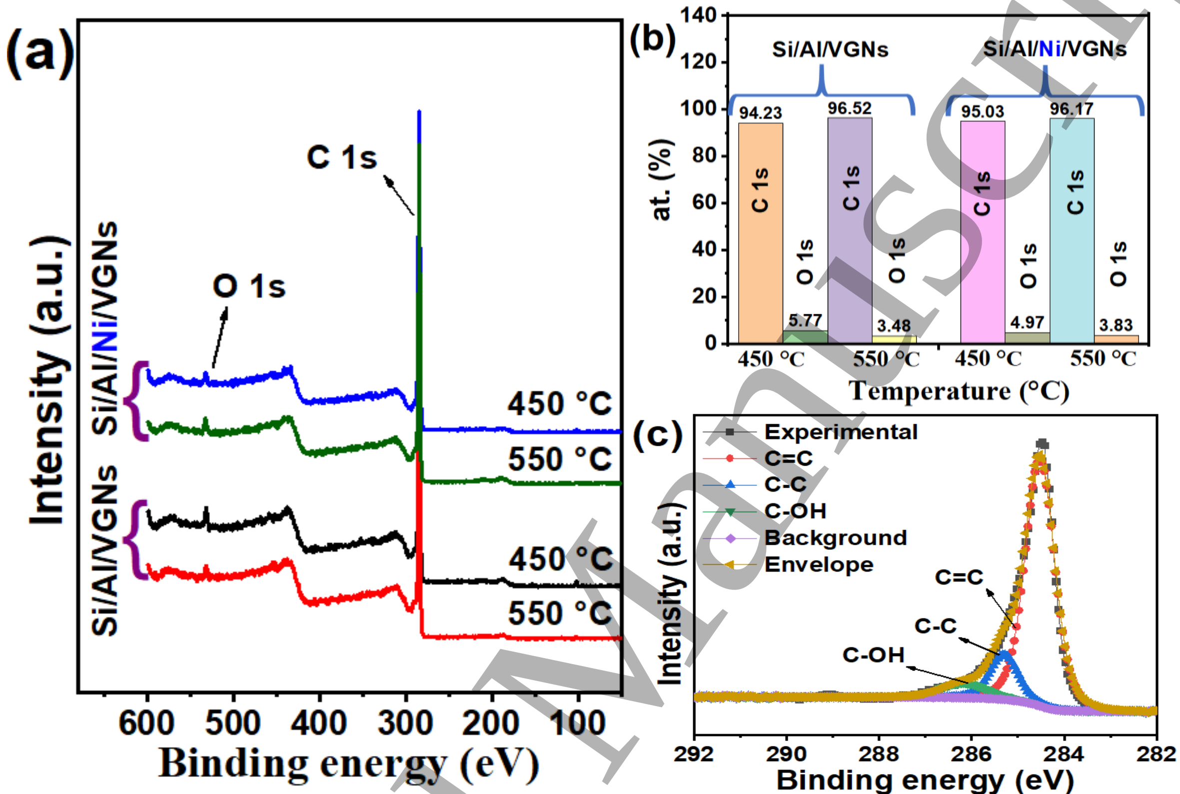

Figure 4. (a) Survey scan comparison of VGNs grown under different conditions (Excitation energy 700 eV), (b) plot of oxygen content in the near-surface region, (c) C 1s deconvoluted spectra of VGNs grown at 550 °C on Si/Al/Ni (excitation energy 385 eV).

Table 1. *Percentage area of the different carbon species obtained from fits of XPS C 1s spectra.*

	(° C)	284.5 eV (%)	285.2 eV (%)	286.1 eV (%)
Si/Al/ VGNs	450	70.5	21.9	7.6
	550	80.1	13.3	6.6
Si/Al/Ni/ VGNs	450	71.4	19.4	9.2
	550	78.9	13.6	7.5

Accepted Manuscript

C 1s of all the samples were deconvoluted into three peaks, as summarized in table 1. The main peak at 284.5 ± 0.2 eV corresponds to sp^2-hybridized graphite-like carbon atoms (C=C), the peak centered at 285.20 ± 0.2 eV is an indication of sp^3-hybridized carbon atoms (C–C) considered to originate from edges, bending, (a-C) absorbed on the graphene surface and the peak at 286.2 ± 0.2 eV is due to OH functional groups attached to carbon atoms (C-OH) [53,54]. It was observed with an increase in growth temperature of VGNs, sp^2 content increases, and sp^3 decreased. These findings also support the interpretation of the results in the Raman analysis that the increase in the D band intensity is due to the boundary edges of graphene sheets and not from defects.

To investigate the growth of VGNs at very low temperatures, the experiment conducted at 410 °C. There is no growth of VGNs observed at these experimental conditions. However, carbon nanoparticles with graphitic characteristics are deposited on the substrate, as observed by the SEM and Raman analysis (figure 5 (a) and (b)). XPS analysis presented in figure 5 (c, d) indicates the significant presence of the nickel and substrate material along with the deposited carbon nanomaterial.

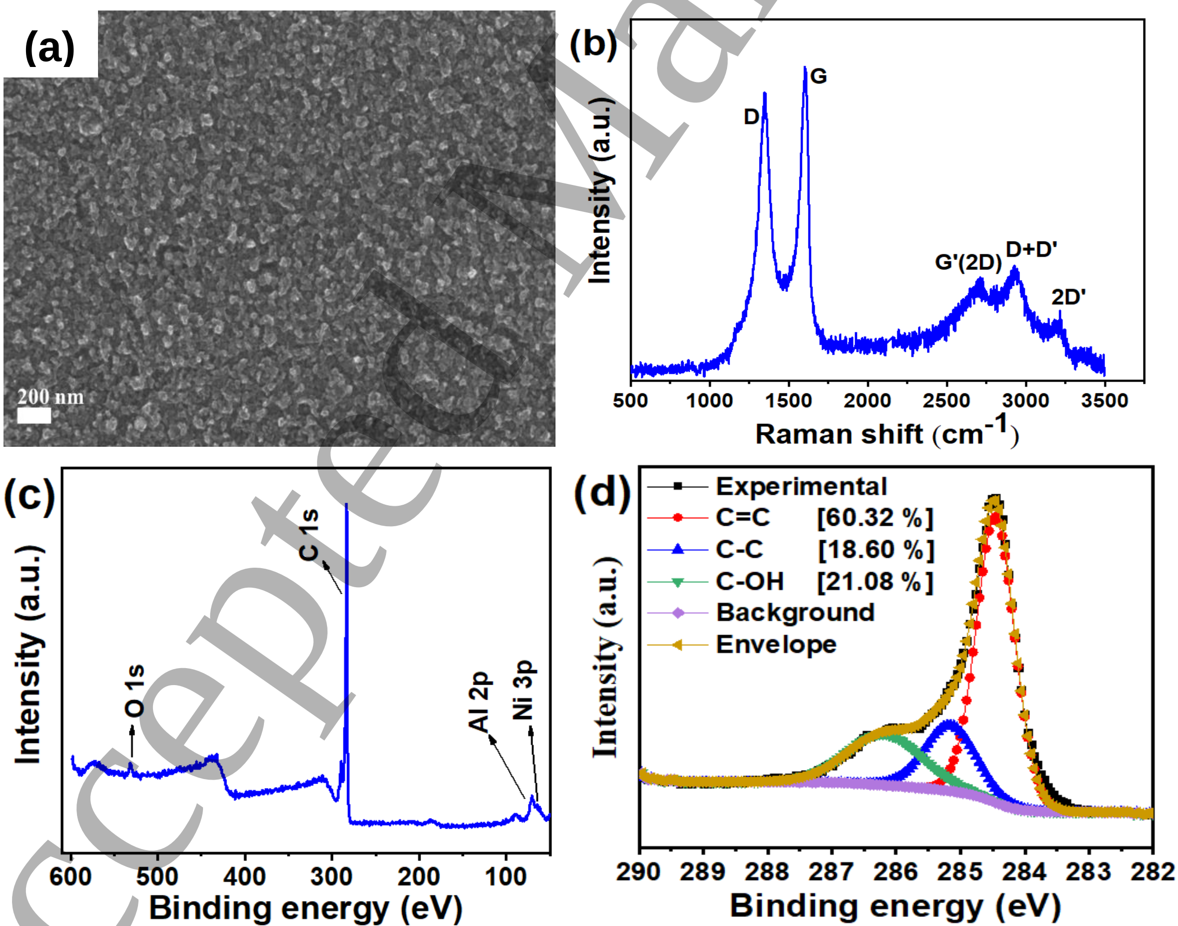

Figure 5. Carbon nanostructures grown at 410 °C on Si/Al/Ni, (a) SEM image, (b) Raman Spectra, (c) XPS survey scan, (d) C 1s deconvoluted spectra.

Accepted Manuscript

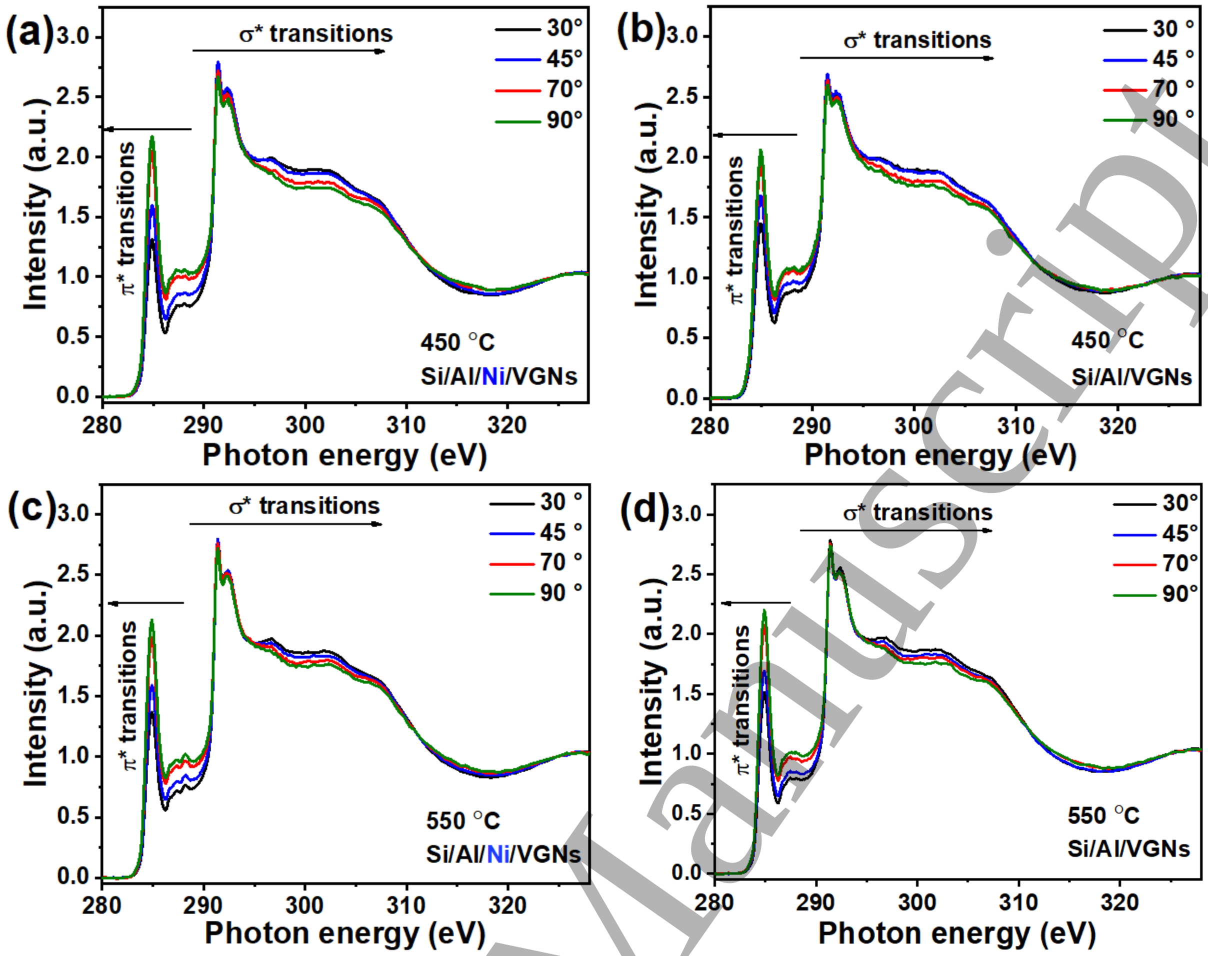

Figure 6. NEXAFS spectra of VGNs grown at 450 °C {(a) with and (b) without nickel as a catalyst}, at 550 °C {(c) With and (d) without nickel as a catalyst}. Angular dependence. All the spectra were normalized to an absorption edge jump setting the post-edge intensity at 325 eV to 1.

Near Edge X-ray Absorption Fine Structure spectroscopy (NEXAFS) is used to lighten up more detailed chemical, structural, and orientation information about VGNs. The spectra were obtained at the C K-edge, in a partial energy electron yield (PEY) mode, with only -20 V of retarding potential. Raw spectra were divided by the absorption spectra of a clean, freshly sputtered gold sample to correct for the photon flux [55]. The energy calibration was obtained by using an I_0 feature referenced to a C 1s →π* resonance at 284.9 eV from a fresh surface of graphite foil standard sample [56]. Spectra are shown after normalization of the edge-step to one. The spectra were collected at different angles (30-90°) of the incident linearly polarized synchrotron-light beam relative to the surface plane of the sample.

Accepted Manuscript

The C K edge NEXAFS spectra of the four samples (VGNs grown at two different temperatures 450 °C and 550 °C) are quite similar to each other and represented in Figure 6 (a-d). Figures (6) show three main absorption features for all the samples, a sharp resonance at about 285.2 eV and a double-structure resonance at around 292 eV. The feature at 285.2 eV is commonly assigned to C 1s to π* transition of sp^2 carbons in a carbon-ring structure, and the features at 291.7 and 292.7 eV can be assigned to double resonances that come from excitonic and band-like contributions of graphitic carbon species, respectively [57–59]. Furthermore, when Ni is added as a catalyst, a small feature at around 288.5 eV becomes more prominent (figure 6 (a)). This change can be attributed to defect states resulting from oxygenated groups and/or surface contaminations on VGNs, e.g., π*C=O, σ* C-H and –(HO-π*C=O) transitions [53,55,60–62] which is also confirmed by XPS analysis (see Table 1).

For all four samples, there is a clear angular dependence of the C1s → π * transition at around 285.2 eV. The differences are strongly correlated with the orientation of the transition dipole moments into the π * orbitals relative to the surface and therefore support the synthesis of VGNs consisting of graphene sheets that grow preferentially perpendicular to the substrate. In this case, by looking to the spectra presented in figure (6), the π* orbitals deriving from p_z orbitals are preferentially oriented parallel to the substrate, and thus the σ* orbitals (in-plane graphene bonds) are oriented perpendicular to the substrate. Therefore, as the angle between the incident beam and surface increases, the C1s → π* resonance at 285.2 eV increases, which validates the SEM images of the respective samples, i.e., preferentially vertically oriented graphene nanosheets have been successfully synthesized.

Thus, comprehensive studies on all the aforementioned results suggesting that VGNs growth is initiated at the lowest temperature of 450 °C and show a perfect structure with an increase in temperature. The presence of Ni catalyst enhances the growth rate and improves the interconnected feature of graphene nanosheets to perfectly orient on the substrate surface.

4. Conclusions

Vertical graphene nanosheets were deposited by radio frequency capacitively coupled plasma. SEM, Raman, XPS, and NEXAFS results affirm the growth of VGNs at the lowest substrate temperature of 450 °C. The use of Ni catalyst on the substrate significantly reduced the nucleation temperature and raised the quality and growth rate of VGNs in comparison to the substrates without Ni. Moreover, the increase in I_D/I_G ratios and D band intensities indicated the improvement in the structural order of graphene nanosheets with increase in synthesis

Accepted Manuscript

temperature. Furthermore, the sp^2 to the sp^3 ratio increased with an increase in the synthesis temperature. These results are further supported by NEXAFS analysis which demonstrated that Ni catalyst facilitates the growth of 2D VGNs at lower temperatures, which opens new horizons for the direct growth of vertical graphene on different substrates at low temperatures with application-oriented properties.

Acknowledgements.

The authors want to thank HZB for the allocation of synchrotron radiation beam time at Bessy II via projects 17205612ST/R, 17206156ST, 18106986ST, 191-07892-ST/R, and 191-08281 ST/R as well as Professor Dr. Ch. Woell, Dr. A. Nefedov for providing the end station and A. Wagner for fruitful discussions. The authors would also like to acknowledge the financial support provided by the French Research Agency through the project ANR PlasBioSens and the Region Centre through the project APR Capt'eau. UC and NMS acknowledge support of Slovenian Research Agency grant no. N2-0091. This work was partially supported by the European Union's Horizon 2020 research and innovation program (PEGASUS H2020-FETOPEN-01-2016-201-RIA 766894).

References.

[1] Mao S, Yu K, Chang J, Steeber D A, Ocola L E and Chen J 2013 Direct Growth of Vertically-oriented Graphene for Field-Effect Transistor Biosensor *Sci. Rep.* **3** 1696

[2] Wu Y, Yang B, Zong B, Sun H, Shen Z and Feng Y 2004 Carbon nanowalls and related materials *J. Mater. Chem.* **14** 469

[3] Wu Y, Qiao P, Chong T and Shen Z 2002 Carbon nanowalls grown by microwave plasma enhanced chemical vapor deposition *Adv. Mater.* **14** 64–7

[4] Hiramatsu M and Hori M 2010 Carbon nanowalls synthesis and emerging applications. DOI 10.1007/978-3-211-99718-5

[5] Russo P, Xiao M and Zhou N Y 2017 Carbon nanowalls: A new material for resistive switching memory devices *Carbon* **120** 54–62

[6] Lehmann K, Yurchenko O, Melke J, Fischer A and Urban G 2018 High electrocatalytic activity of metal-free and non-doped hierarchical carbon nanowalls towards oxygen reduction reaction *Electrochimica Acta* **269** 657–667

[7] Evlashin S A, Maksimov Y M, Dyakonov P V., Pilevsky A A, Maslakov K I, Mankelevich Y A, Voronina E N, Vavilov S V., Pavlov A A, Zenova E V., Akhatov I S and Suetin N V. 2019 N-Doped Carbon NanoWalls for Power Sources *Sci. Rep.* **9** 6716

Accepted Manuscript

[8] Guzmán-Olivos F, Espinoza-González R, Fuenzalida V and Morell G 2019 Field emission properties of carbon nanowalls prepared by RF magnetron sputtering *Appl. Phys. A* **125** 354

[9] Kumar S, Martin P, Bendavid A, Bell J and Ostrikov Kostya (Ken) 2019 Oriented graphenes from plasma-reformed coconut oil for supercapacitor electrodes Nanomaterials **9** 1679

[10] Yen H-F F, Horng Y-Y Y, Hu M-S S, Yang W-H H, Wen J-R R, Ganguly A, Tai Y, Chen K-H H and Chen L-C C 2015 Vertically aligned epitaxial graphene nanowalls with dominated nitrogen doping for superior supercapacitors *Carbon N. Y.* **82** 124–34

[11] Ghosh S, Ganesan K, Polaki S R, Mathews T, Dhara S, Kamruddin M and Tyagi A K 2015 Influence of substrate on nucleation and growth of vertical graphene nanosheets *Appl. Surf. Sci.* **349** 576–81

[12] Fang J, Levchenko I, Kumar S, Seo D and Ostrikov Kostya (Ken) 2014 Vertically aligned graphene flakes on nanoporous templates: morphology, thickness, and defect level control by pretreatment *Sci. Technol. Adv. Mater*. **15** 055009 (8pp).

[13] Hiramatsu M, Nihashi Y, Kondo H and Hori M 2013 Nucleation Control of Carbon Nanowalls Using Inductively Coupled Plasma-Enhanced Chemical Vapor Deposition *Jpn. J. Appl. Phys.* **52** 01AK05

[14] Malesevic A, Vitchev R, Schouteden K, Volodin A, Zhang L, Tendeloo G Van, Vanhulsel A and Haesendonck C Van 2008 Synthesis of few-layer graphene via microwave plasma-enhanced chemical vapour deposition *Nanotechnology* **19** 305604

[15] Krivchenko V, Shevnin P, Pilevsky A, Egorov A, Suetin N, Sen V, Evlashin S and Rakhimov A 2012 Influence of the growth temperature on structural and electron field emission properties of carbon nanowall/nanotube films synthesized by catalyst-free PECVD *J. Mater. Chem.* **22** 16458

[16] Hori M, Kondo H and Hiramatsu M 2011 Radical-controlled plasma processing for nanofabrication. *J. Phys. D: Appl. Phys* **44** 174027 (15pp).

[17] Shiji K, Hiramatsu M, Enomoto A, Nakamura M, Amano H and Hori M 2005 Vertical growth of carbon nanowalls using rf plasma-enhanced chemical vapor deposition *Diam. Relat. Mater.* **14** 831–4

[18] Hiramatsu M and Hori M. 2010 Carbon Nanowalls. Chapter 2 Preparation Methods. DOI 10.1007/978-3-211-99718-5_2, # Springer-Verlag/Wien pp 9–30

[19] Bo Z, Yang Y, Chen J, Yu K, Yan J and Cen K 2013 Plasma-enhanced chemical vapor deposition synthesis of vertically oriented graphene nanosheets *Nanoscale* **5** 5180

Accepted Manuscript

[20] Santhosh N, Filipič G, Tatarova E, Baranov O, Kondo H, Sekine M, Hori M, Ostrikov K and Cvelbar U 2018 Oriented Carbon Nanostructures by Plasma Processing: Recent Advances and Future Challenges *Micromachines* **9** 565

[21] Park J K, Kang H, Kim J H and Choi W 2018 Improvement of Electrical Properties of Carbon Nanowall by the Deposition of Thin Film *J. Nanosci. Nanotechnol.* **18** 6026–8

[22] Giese A, Schipporeit S, Buck V and Wöhrl N 2018 Synthesis of carbon nanowalls from a single-source metal-organic precursor *Beilstein J. Nanotechnol.* **9** 1895–905

[23] Bo Z, Yu K, Lu G, Wang P, Mao S and Chen J 2011 Understanding growth of carbon nanowalls at atmospheric pressure using normal glow discharge plasma-enhanced chemical vapor deposition *Carbon N. Y.* **49** 1849–58

[24] Mori T, Hiramatsu M, Yamakawa K, Takeda K and Hori M 2008 Fabrication of carbon nanowalls using electron beam excited plasma-enhanced chemical vapor deposition *Diam. Relat. Mater.* **17** 1513–7

[25] Hiramatsu M, Shiji K, Amano H and Hori M 2004 Fabrication of vertically aligned carbon nanowalls using capacitively coupled plasma-enhanced chemical vapor deposition assisted by hydrogen radical injection *Appl. Phys. Lett.* **84** 4708–10

[26] Kondo S, Kawai S, Takeuchi W, Yamakawa K, Den S, Kano H, Hiramatsu M and Hori M 2009 Initial growth process of carbon nanowalls synthesized by radical injection plasma-enhanced chemical vapor deposition *J. Appl. Phys.* **106** 094302

[27] Yang Q, Wu J, Li S, Zhang L, Fu J, Huang F F and Cheng Q 2019 Vertically-oriented graphene nanowalls: Growth and application in Li-ion batteries *Diamond & Related Materials* **91** 54–63.

[28] Wang J, Zhu M, Outlaw R A A, Zhao X, Manos D M M and Holloway B C C 2004 Synthesis of carbon nanosheets by inductively coupled radio-frequency plasma enhanced chemical vapor deposition *Carbon N. Y.* **42** 2867–72

[29] Malesevic A, Vizireanu S, Kemps R, Vanhulsel A, Haesendonck C V and Dinescu G 2007 Combined growth of carbon nanotubes and carbon nanowalls by plasma-enhanced chemical vapor deposition *Carbon* **45** 2932–2937

[30] Vizireanu S, Mitu B, Luculescu C R, Nistor L C and Dinescu G 2012 PECVD synthesis of 2D nanostructured carbon material *Surf. Coatings Technol.* **211** 2–8

[31] Labbaye T, Kovacevic E, Lecas T, Ammar M R, Canizarès A, Raimboux N, Strunskus T, Jaeger C, Simon P and Boulmer-Leborgne C 2018 Enhancement of catalytic effect for CNT growth at low temperature by PECVD *Applied Surface Science* **453** 436–441

[32] Esconjauregui S, Bayer B C C, Fouquet M, Wirth C T T, Ducati C, Hofmann S and

Accepted Manuscript

Robertson J 2009 Growth of high-density vertically aligned arrays of carbon nanotubes by plasma-assisted catalyst pretreatment *Appl. Phys. Lett.* **95** 173115

[33] Khalilov U, Bogaerts A, Hussain S, Kovacevic E, Brault P, Boulmer-Leborgne C and Neyts E C 2017 Nanoscale mechanisms of CNT growth and etching in plasma environment *J. Phys. D. Appl. Phys.* **50** 184001

[34] Pattyn C, Kovacevic E, Hussain S, Dias A, Lecas T and Berndt. J. 2018 Nanoparticle formation in a low pressure argon/aniline RF plasma *Appl. Phys. Lett*. **112** 013102

[35] Hussain S, Kovacevic E, Amade R, Berndt J, Pattyn C, Dias A, Boulmer-Leborgne C, Ammar M R and Bertran-Serra E 2018 Plasma synthesis of polyaniline enrobed carbon nanotubes for electrochemical applications. *Electrochimica Acta*. **268** 218–225.

[36] Labbaye T, Canizares A, Gaillard M, Lecas T, Kovacevic E, Ch Boulmer-Leborgne, Strunskus T, Raimboux N, Simon P, Guimbretiere G and Ammar M R 2014 In situ Raman spectroscopy for growth monitoring of vertically aligned multiwall carbon nanotubes in plasma reactor, Appl. Phys. Lett. **105** 213109.

[37] Gaillard M, Boulmer-Leborgne C, Semmar N, Millon É and Petit A 2012 Carbon nanotube growth from metallic nanoparticles deposited by pulsed-laser deposition on different substrates *Appl. Surf. Sci.* **258** 9237–41

[38] Girard-Lauriault P-L, Ruiz J-C, Gross T, Wertheimer M R and Unger W E S 2011 Ultra-Shallow Chemical Characterization of Organic Thin Films Deposited by Plasma and Vacuum-Ultraviolet, Using Angle- and Excitation Energy-Resolved XPS *Plasma Chem. Plasma Process.* **31** 535–50

[39] Maslova O A, Ammar M R, Guimbretiere G, Rouzaud J.-N and Simon P 2012 Determination of crystallite size in polished graphitized carbon by Raman spectroscopy. *Physical Review*. **86** 134205

[40] Ammar M R, Charon E, Rouzaud J.-N, Aleon J, Guimbretiere G and Simon P 2011 On a reliable structural characterization of polished carbons in meteorites by Raman Microspectroscopy *Spectroscopy Letters*. **44** 535–538

[41] Park J S, Reina A, Saito R, Kong J, Dresselhaus G and Dresselhaus M S 2009 G' band Raman spectra of single, double and triple layer graphene. *Carbon* **47** 1303–1310

[42] Pimenta A, Dresselhaus G, Dresselhaus M S, Cancado L G, Jorio A and Saito R 2007 Studying disorder in graphite-based systems by Raman spectroscopy. *Physical Chem. Chem. Phys*. **9** 1276–1290

[43] Ghosh S, Ganesan K, Polaki S R, Ravindran T R, Krishna N G, Kamruddin M and Tyagi A K 2014 Evolution and defect analysis of vertical graphene nanosheets *J. Raman*

Accepted Manuscript

Spectrosc.

[44] Yang C, Bi H, Wan D, Huang F, Xie X and Jiang M 2013 Direct PECVD growth of vertically erected graphene walls on dielectric substrates as excellent multifunctional electrodes *J. Mater. Chem. A* **1** 770–5

[45] Tuinstra F and Koenig J L 1970 Raman Spectrum of Graphite *J. Chem. Phys.* **53** 1126–30

[46] Ammar M R, Galy N, Rouzaud J N, Toulhoat N, Vaudey C E, Simon P and Moncoffre N 2015 Characterizing various types of defects in nuclear graphite using Raman scattering: Heat treatment, ion irradiation and polishing *Carbon N. Y.* **95** 364–73

[47] Kurita S, Yoshimura A, Kawamoto H, Uchida T, Kojima K, Tachibana M, Molina-Morales P and Nakai H 2005 Raman spectra of carbon nanowalls grown by plasma-enhanced chemical vapor deposition *J. Appl. Phys.* **97** 104320

[48] Cançado L G, Takai K, Enoki T, Endo M, Kim Y A, Mizusaki H, Jorio A, Coelho L N, Magalhães- Paniago R and Pimenta M A 2006 General equation for the determination of the crystallite size of nanographite by Raman spectroscopy. Appl. Phys. Lett. **88**, 163106.

[49] Knight D S and White W B 1989 Characterization of diamond films by Raman spectroscopy *J. Mater. Res.* **4** 385–93

[50] Lucchese M M, Stavale F, Martins Ferreira E H, Vilani C, Moutinho M V O, Capaz R B, Achete C A and Jorio A 2010 Quantifying ion-induced defects and Raman relaxation length in graphene *Carbon* **48** 1592–1597

[51] Kondo H, Takeuchi W, Hori M, Kimura S, Kato Y, Muro T, Kinoshita T, Sakata O, Tajiri H and Hiramatsu M 2011 Synchrotron x-ray analyses of crystalline and electronic structures of carbon nanowalls. *Appl. Phys. Lett*. **99** 213110

[52] M. Santhosh N, Filipič G, Kovacevic E, Jagodar A, Berndt J, Strunskus T, Kondo H, Hori M, Tatarova E and Cvelbar U 2020 N-Graphene Nanowalls via Plasma Nitrogen Incorporation and Substitution: The Experimental Evidence *Nano-Micro Lett.* **12** 53

[53] Yueh C L, Jan J C, Chiou J W, Pong W F, Tsai M H, Chang Y K, Chen Y Y, Lee Y F, Tseng P K, Wei S L, Wen C Y, Chen L C and Chen K H 2001 Electronic structure of the Fe-layer-catalyzed carbon nanotubes studied by x-ray-absorption spectroscopy *Appl. Phys. Lett.* **79** 3179–81

[54] Okpalugo T I T, Papakonstantinou P, Murphy H, McLaughlin J and Brown N M D 2005 High resolution XPS characterization of chemical functionalized MWCNTs and SWCNTs. *Carbon* **43**, 153–161

Accepted Manuscript

[55] J Stöhr. (1992) NEXAFS Spectroscopy. Springer, Berlin. http://dx.doi.org/10.1007/978-3-662-02853-7

[56] Schmidt C, Breuer T, Wippermann S, Schmidt W G and Witte G 2012 Substrate induced thermal decomposition of perfluoro-pentacene thin films on the coinage metals. *J. Phys. Chem. C*. **116** *45* 24098–24106.

[57] Tatarova E, Dias A, Henriques J, Abrashev M, Bundaleska N, Kovacevic E, Bundaleski N, Cvelbar U, Valcheva E, Arnaudov B, Do Rego A M B B, Ferraria A M, Berndt J, Felizardo E, Teodoro O M N D N D, Strunskus T, Alves L L and Gonçalves B 2017 Towards large-scale in free-standing graphene and N-graphene sheets *Sci. Rep.* **7** 10175

[58] Ehlert C, Unger W E S and Saalfrank P 2014 C K-edge NEXAFS spectra of graphene with physical and chemical defects: a study based on density functional theory *Phys. Chem. Chem. Phys.* **16** 14083–95

[59] Zhang W, Nefedov A, Naboka M, Cao L and Wool C 2012 Molecular orientation of terephthalic acid assembly on epitaxial graphene: NEXAFS and XPS study. *Phys Chem. Chem. Phys* **14** 10125–10131

[60] Fischer D A, Wentzcovitch R M, Carr R G, Continenza A and Freeman A J 1991 Graphitic interlayer states: A carbon K near-edge x-ray-absorption fine-structure study *Phys. Rev. B* **44** 1427–9

[61] Mane J M, Normand François Le, Medjo R E, Cojocaru C S, Ersen O, Senger A, Laffon C, Sendja B T, Biouele C M, Ben-Bolie G H, Ateba P O and Parent P 2014 Alignment of vertically grown carbon nanostructures studied by X-Ray absorption spectroscopy. *Materials Sciences and Applications* **5** 966–983

[62] Babaa M R, Bantignies J L, Alvarez L, Parent P, Normand F Le, Gulas M, Mane K Mane, Poncharal P and Doyle B P 2007 NEXAFS study of multi-walled carbon nanotubes functionalization with sulfonated Poly(ether ketone) chains *Journal of Nanoscience and Nanotechnology* **7** 3463–3467

Accepted Manuscript